



THE UNIVERSITY *of* EDINBURGH

Edinburgh Research Explorer

Danger signals activate a putative innate immune system during regeneration in a filamentous fungus

Citation for published version:

Medina-Castellanos, E, Villalobos-Escobedo, JM, Riquelme, M, Read, ND, Abreu-Goodger, C & Herrera-Estrella, A 2018, 'Danger signals activate a putative innate immune system during regeneration in a filamentous fungus', *PLoS Genetics*. <https://doi.org/10.1371/journal.pgen.1007390>

Digital Object Identifier (DOI):

[10.1371/journal.pgen.1007390](https://doi.org/10.1371/journal.pgen.1007390)

Link:

[Link to publication record in Edinburgh Research Explorer](#)

Document Version:

Publisher's PDF, also known as Version of record

Published In:

PLoS Genetics

General rights

Copyright for the publications made accessible via the Edinburgh Research Explorer is retained by the author(s) and / or other copyright owners and it is a condition of accessing these publications that users recognise and abide by the legal requirements associated with these rights.

Take down policy

The University of Edinburgh has made every reasonable effort to ensure that Edinburgh Research Explorer content complies with UK legislation. If you believe that the public display of this file breaches copyright please contact openaccess@ed.ac.uk providing details, and we will remove access to the work immediately and investigate your claim.



RESEARCH ARTICLE

Danger signals activate a putative innate immune system during regeneration in a filamentous fungus

Elizabeth Medina-Castellanos¹✉, José Manuel Villalobos-Escobedo¹✉, Meritxell Riquelme², Nick D. Read³, Ceil Abreu-Goodger¹✉, Alfredo Herrera-Estrella¹*

1 Laboratorio Nacional de Genómica para la Biodiversidad-Unidad de Genómica Avanzada, Cinvestav, Libramiento Norte Carretera Irapuato-León, Irapuato, Gto, Mexico, **2** Department of Microbiology, Centro de Investigación Científica y de Educación Superior de Ensenada (CICESE), Carretera Ensenada-Tijuana No. 3918, Ensenada, Baja California, Mexico, **3** Manchester Fungal Infection Group, Division of Infection, Immunity and Respiratory Medicine, University of Manchester, Manchester, United Kingdom

✉ These authors contributed equally to this work.

* alfredo.herrera@cinvestav.mx.



OPEN ACCESS

Citation: Medina-Castellanos E, Villalobos-Escobedo JM, Riquelme M, Read ND, Abreu-Goodger C, Herrera-Estrella A (2018) Danger signals activate a putative innate immune system during regeneration in a filamentous fungus. *PLoS Genet* 14(11): e1007390. <https://doi.org/10.1371/journal.pgen.1007390>

Editor: A. Aziz Aboobaker, University of Oxford, UNITED KINGDOM

Received: May 2, 2018

Accepted: October 19, 2018

Published: November 30, 2018

Copyright: © 2018 Medina-Castellanos et al. This is an open access article distributed under the terms of the [Creative Commons Attribution License](https://creativecommons.org/licenses/by/4.0/), which permits unrestricted use, distribution, and reproduction in any medium, provided the original author and source are credited.

Data Availability Statement: The RNAseq data discussed in this manuscript have been deposited in NCBI's Gene Expression Omnibus and are accessible through GEO Series accession number GSE115811 (<https://www.ncbi.nlm.nih.gov/geo/query/acc.cgi?acc=GSE115811>).

Funding: EMC and JMVE are indebted to Consejo Nacional de Ciencia y Tecnología (CONACYT) for doctoral fellowships. EMC received a short stay fellowship from CONACYT. This work was

Abstract

The ability to respond to injury is a biological process shared by organisms of different kingdoms that can even result in complete regeneration of a part or structure that was lost. Due to their immobility, multicellular fungi are prey to various predators and are therefore constantly exposed to mechanical damage. Nevertheless, our current knowledge of how fungi respond to injury is scarce. Here we show that activation of injury responses and hyphal regeneration in the filamentous fungus *Trichoderma atroviride* relies on the detection of two danger or alarm signals. As an early response to injury, we detected a transient increase in cytosolic free calcium ($[Ca^{2+}]_c$) that was promoted by extracellular ATP, and which is likely regulated by a mechanism of calcium-induced calcium-release. In addition, we demonstrate that the mitogen activated protein kinase Tmk1 plays a key role in hyphal regeneration. Calcium- and Tmk1-mediated signaling cascades activated major transcriptional changes early following injury, including induction of a set of regeneration associated genes related to cell signaling, stress responses, transcription regulation, ribosome biogenesis/translation, replication and DNA repair. Interestingly, we uncovered the activation of a putative fungal innate immune response, including the involvement of HET domain genes, known to participate in programmed cell death. Our work shows that fungi and animals share danger-signals, signaling cascades, and the activation of the expression of genes related to immunity after injury, which are likely the result of convergent evolution.

Author summary

The idea of regenerating lost body parts has always fascinated humans due to its impact on human health. Recently, the study of the response to damage has gained importance not only in regenerative medicine, but also in organ transplantation. We have established a microbial model that given its relative simplicity and ease to work with, promises to

supported by CONACYT grant - Investigación en Fronteras de la Ciencia (FON.INST./117/2016) to AHE <https://www.conacyt.gob.mx/> and the CABANA project, which is funded by the BBSRC under the The Global Challenges Research Fund (GCRF) Growing Research Capability call, contract number BB/P027849/1 (www.ukri.org/research/global-challenges-research-fund/funded-projects/). The funders had no role in study design, data collection and analysis, decision to publish, or preparation of the manuscript.

Competing interests: The authors have declared that no competing interests exist.

accelerate the advance of our understanding of damage responses and regeneration. We show that activation of injury responses and hyphal regeneration in a filamentous fungus relies on the detection of danger (also called alarm) signals also used by plants and animals. Finally, we discovered a set of genes that become active in response to injury, including those putatively participating in the immune response.

Introduction

The idea of regenerating lost body parts has fascinated humans since the beginning of history [1]. Human imagination was further captured upon witnessing the extraordinary capacity of species from almost all Phyla to, upon damage, regenerate a lost part or structure [1]. Nevertheless, our understanding of the biological significance and molecular mechanisms underpinning this remarkable phenomenon and its evolution is still poor.

Multicellular organisms establish interactions with a great variety of other, potentially harmful, organisms throughout their life. Consequently, they require mechanisms to detect injury and to distinguish self- from non-self. Discrimination of self/non-self is a ubiquitous and essential function, which in animals relies on the immune system. Similarly, multicellular organisms require alarm signals known as Damage-Associated Molecular Patterns (DAMPs) to contend with a wound. In this regard, normal cellular components released into extracellular spaces, such as DNA, ATP and Ca^{2+} , represent reliable signals that indicate to other cells the disruption of tissue, and trigger a response [2]. Intracellular signaling after injury involves Mitogen Activated Protein Kinases (MAPKs), as in the case of axon regeneration after spinal cord injury in vertebrates [3] and herbivory in plants [4].

Plant and animal cells have the ability to detect extracellular ATP (eATP) through recognition by specific, yet unrelated, receptors [2,5,6]. Activation of purinergic receptors or mechano-sensors triggers a transient increase in intracellular Ca^{2+} [7, 8]. In plants, eATP promotes calcium influxes after wounding [9] and large increases in eATP serve as a key “danger” signals in the inflammatory processes of zebrafish and humans [8, 10]. In animals, danger signals activate genes involved in cell signaling, stress responses, tissue patterning, cell matrix remodeling and growth [11–13]. Reactive Oxygen Species (ROS) are also considered as danger signals in plants and animals, and necessary to prevent infections during wound healing [2]. Sustained production of ROS is required for regeneration in *Xenopus* and zebrafish [14,15]. Furthermore, ROS is involved in the regulation of intracellular Ca^{2+} levels [16].

During tissue regeneration, a competent immune system is essential for effective wound healing [17]. Common features of innate immunity in vertebrates, invertebrate and plants include the basic chemical structure of signal molecules, signaling cascades, production of antimicrobial molecules, and transcriptional activation of defense genes [2, 18].

Fungi like other organisms have natural predators, including fungivorous nematodes and arthropods, consequently they need effective mechanisms to contend with and survive injury. When fungal hyphae are damaged, the septal pore nearest to the point of injury is sealed to prevent excessive cytoplasmic leakage. Thereafter, new hyphal tips are generated from this position, resulting in regeneration and re-initiation of growth [18].

The common soil fungus *Trichoderma atroviride* responds to mycelial injury by rapidly regenerating its hyphae and, developing asexual reproductive structures (conidia) in a NADPH oxidase (Nox) dependent manner [19]. Interestingly, application of eATP also induces conidiation [20]. Like other multicellular eukaryotes, this fungus appears to perceive eATP, through a yet unidentified receptor, which triggers activation of the MAPKs Tmk1 and

Tmk3 [20]. Tmk3 is activated in a Nox1-NoxR dependent fashion, whereas Tmk1 activation is independent of Nox [20]. Mutants in either *tmk1* or *tmk3* are affected in injury-induced conidiation. Interestingly, depletion of extracellular Ca^{2+} blocked injury-induced conidiation but allowed activation of both MAPKs [20].

In addition to its role in injury-induced conidiation, Tmk3 regulates tolerance to heat shock, osmotic and oxidative stress, and cell wall integrity [21]. Unexpectedly, *tmk3* mutants are also impaired in light-induced conidiation [21]. In contrast Δtmk1 mutants, albeit of a different *T. atroviride* strain, hyperconidiate under standard cultivation conditions [22]. Tmk1 has also been suggested to regulate mycoparasitic activity and hyphal fusion [22, 23].

Here we provide new mechanistic insights into the activation of a regeneration program, consisting of genes involved in cell signaling, stress responses, transcription, ribosome biogenesis/translation, DNA replication, growth, and defense through Ca^{2+} /MAPK-dependent signaling pathways. Finally, we uncover the activation of genes of a putative fungal innate immune response involving genes previously known to participate in heterokaryon incompatibility [24].

Results

Injury induces a transient increase in $[\text{Ca}^{2+}]_c$ that is required for transcriptional regulation of hyphal regeneration

Considering the relevant role of calcium in regeneration in other organisms, we evaluated calcium signatures at wound sites in *T. atroviride*. Live-imaging analysis of wounded cells, expressing the Ca^{2+} sensor GCaMP6, revealed a transient spike of cytosolic free calcium ($[\text{Ca}^{2+}]_c$) immediately after injury (Fig 1A, S1 and S2 Movies). To determine if extracellular calcium was involved in this response, we applied the calcium-chelating agent BAPTA. Injury promoted a transient elevation of $[\text{Ca}^{2+}]_c$, while treatment with BAPTA prior to injury completely suppressed this response (Fig 1A). The injury-induced calcium signature showed a very rapid and strong peak of increase in $[\text{Ca}^{2+}]_c$ that decreased over time (Fig 1B). In contrast, in presence of BAPTA, the $[\text{Ca}^{2+}]_c$ was not altered upon injury (Fig 1B). The decrease in fluorescence observed in the graphs just before injury (indicated by an arrow) is an unavoidable artifact due to the introduction of the scalpel used to cause the injury, which blocks light. To test if the observed response involved uptake of extracellular calcium and/or release of calcium from intracellular pools, we applied the calcium release inhibitors verapamil, which blocks L-type calcium channels in the plasma membrane, and dantrolene that inhibits Ca^{2+} -induced Ca^{2+} release from the sarcoplasmic reticulum pool by targeting the ryanodine receptor [25]. Both compounds significantly reduced $[\text{Ca}^{2+}]_c$ increases due to injury (Fig 1C), consistent with the participation of a calcium-induced calcium release system. Next, we analyzed the role of calcium in the regeneration process. Application of BAPTA to the fungal mycelium prior to injury reduced regenerating hyphae to 20%, as compared to 64% observed in an untreated control (Fig 1D and 1E). Addition of extracellular calcium to hyphae previously exposed to BAPTA partially restored regeneration upon damage, as evidenced by the formation of thin new hyphae as a result of tip growth re-initiation (Fig 1D) and an increase in regeneration (52%; Fig 1E).

We then compared the transcriptional profile of the fungus in response to Injury in the presence (IB) and absence (I) of BAPTA. We identified a total of 421 Calcium-Dependent Injury Genes (CDIGs), responsive only in the absence of BAPTA; of which 241 were up-regulated and 180 down-regulated. In addition, we identified 404 Calcium-Independent Injury Genes (CIIGs), responsive even in the presence of BAPTA; 201 of which were up-regulated and 203 down-regulated (Fig 2A, S1–S3 Datasets). Upon injury, the fungus up-regulates genes associated to the following cellular components: chromosomes, lumen enclosed by membrane,

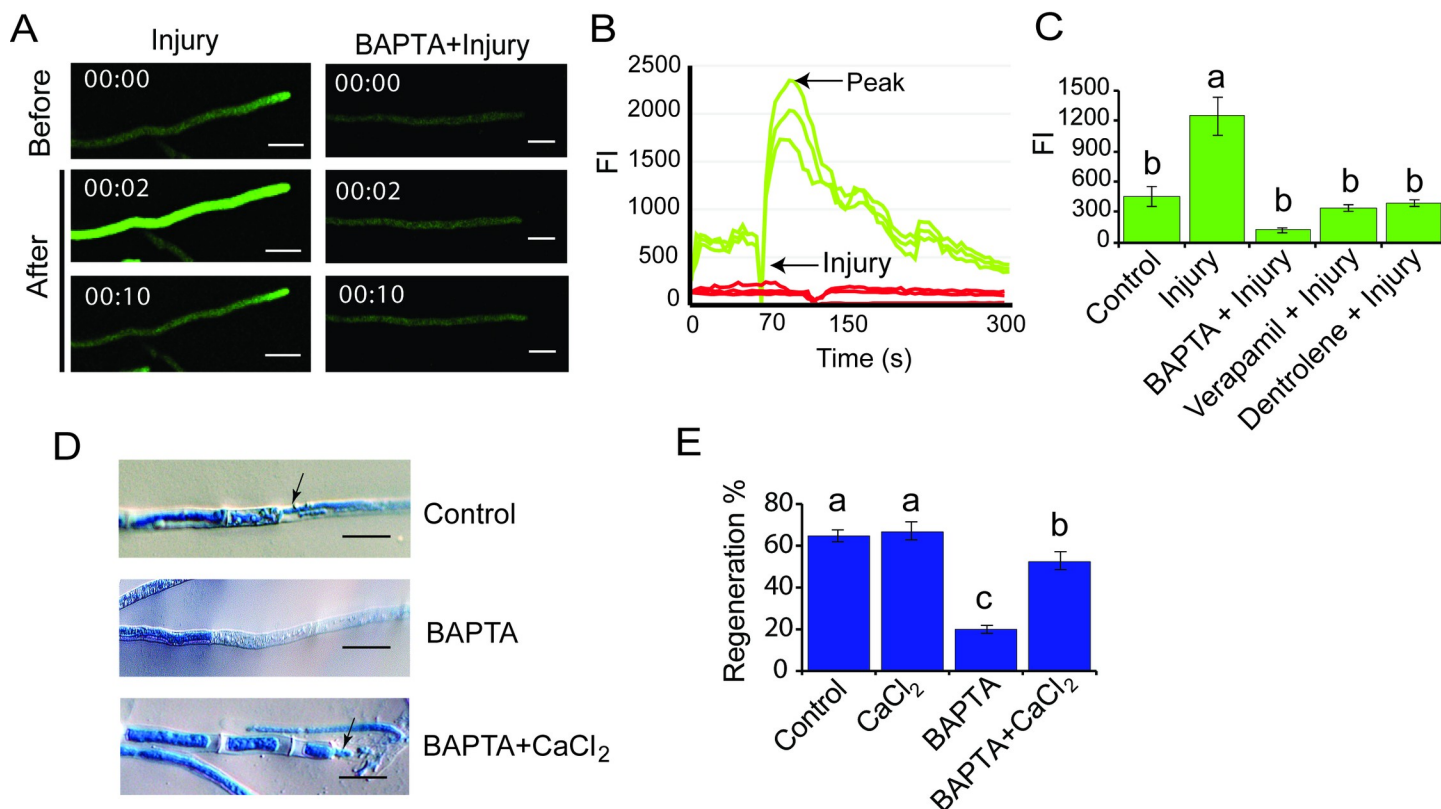


Fig 1. Role of Ca^{2+} in the early response to injury. **A.** Live-cell imaging. The *T. atroviride* WT strain carrying the sensor GCamP6 was damaged with a scalpel, or exposed to BAPTA and then damaged. Images were obtained using time-lapse confocal microscopy. Scale bar = 10 μM . Time shown in seconds. **B.** The graph shows the Fluorescence Intensity (FI) per hypha of the WT strain carrying the sensor GCamP6 for three representative hyphae during injury (green line) and treated with BAPTA and then injured (red lines) for three representative hyphae. **C.** Effect of calcium channels inhibitors on $[\text{Ca}^{2+}]_i$. The graph shows the mean maximum change of FI approximately 2–6 sec after injury. In each case the WT strain was treated with the indicated Ca^{2+} inhibitor before injury. Four independent experiments were performed for each treatment. **D.** Microscopic changes. One hour after injury hyphae were stained with lactophenol cotton blue and examined by light microscopy. Treatments were: Control: normal regeneration response of injured hyphae; BAPTA: hyphae did not regenerate after being exposed to BAPTA for 15 min and then damaged; BAPTA + CaCl_2 : partial restoration of hyphal regeneration following exposure to BAPTA for 15 min and then addition of 0.34 mM CaCl_2 . Arrows point to the new hyphae. Scale bar = 10 μM . **E.** Regeneration capacity. The graph shows the percentage of hyphae that regenerate after each treatment. Three independent experiments were performed for each treatment, counting 50 hyphae in each case. **C, E.** Bars represent the mean \pm s.e.m. A one-way ANOVA test, followed by Tukey Honest Significant Differences was used. Different letters indicate significant differences ($P < 0.05$).

<https://doi.org/10.1371/journal.pgen.1007390.g001>

ribonucleoprotein complexes, intracellular non-membrane-bound organelles (associated with the cytoskeleton) and macromolecular complexes (Fig 2B, WT-I vs WT-C, S4 Dataset). BAPTA chelation of calcium blocked genes that were associated with chromosomes, and non-membrane-bound organelles, but induced genes related to microbodies (vacuoles), apparently in an injury independent fashion (Fig 2B, WT-IB vs WT-C & WT-IB vs WT-I). Moreover, injury caused an increase in genes belonging to the biological processes of RNA processing, translation, DNA metabolic processes and replication (Fig 2C; WT-I vs WT-C). Remarkably, upon injury, but in the absence of extracellular calcium, there was no significant enrichment in these processes (Fig 2C, WT-IB vs WT-C).

eATP is a primary danger signal that induces Ca^{2+} influx and triggers hyphal regeneration

We had previously suggested that eATP could function as a DAMP [20]. To determine if indeed eATP serves as a DAMP that triggers Ca^{2+} influxes in *T. atroviride* after wounding, we

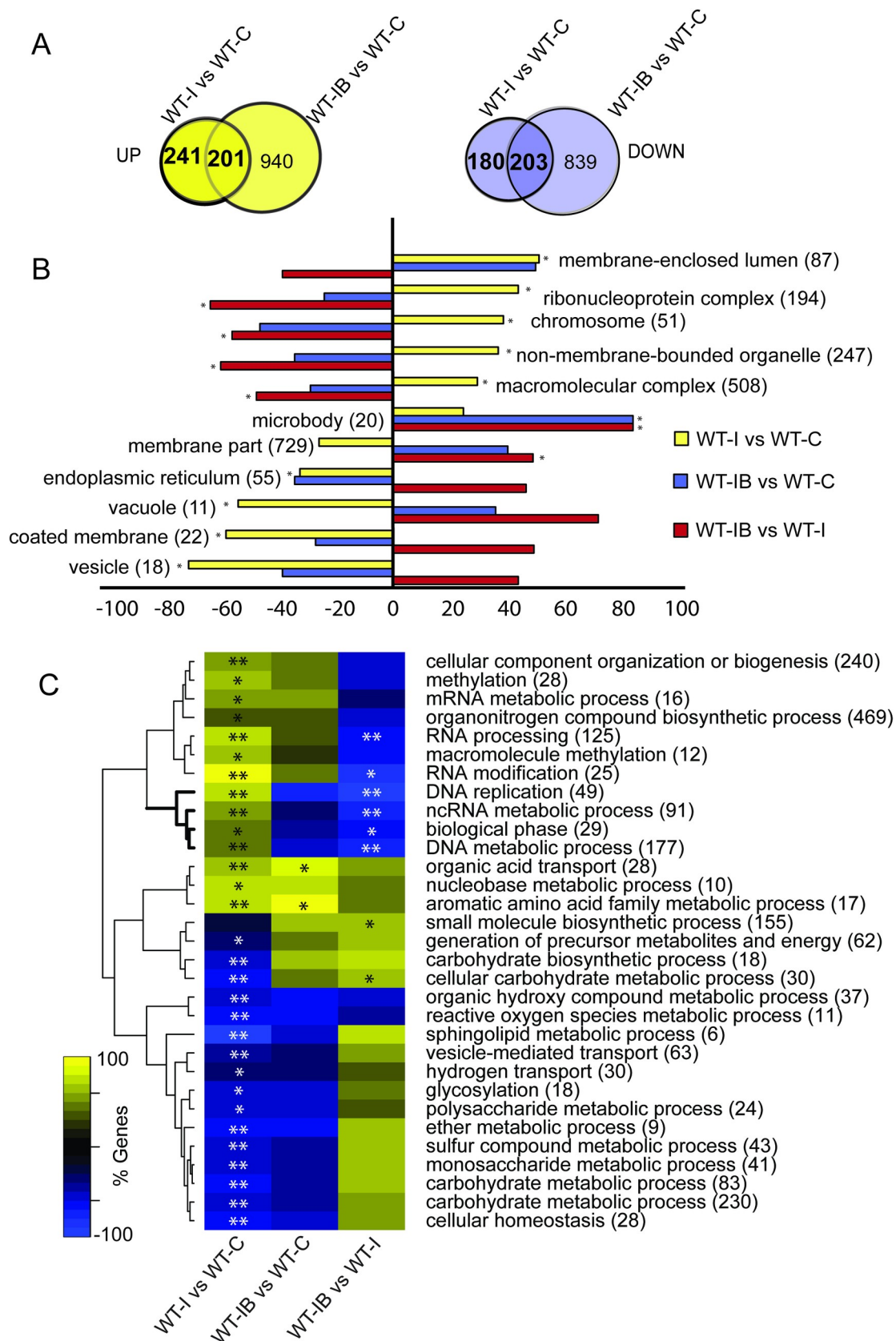


Fig 2. Calcium is essential for the transcriptional response to injury. A. Venn diagrams show the overlap of the induced (yellow) and repressed (purple) genes of the WT strain in response to injury (WT-I) and in response to injury after BAPTA treatment (WT-IB), as compared to an untreated control (WT-C). B. Enrichment analysis using Cellular Component Gene Ontology (GO) terms, showing the percentage of induced or repressed genes belonging to each category (FDR <0.05*). C. Clustering of significantly enriched Biological Process GO terms, showing the percentage of induced or repressed genes belonging to each category (FDR <0.01**; FDR <0.05*). In B and C, the sign indicates the direction of change, positive/negative being higher/lower in injury than in the control. The number in parenthesis after each GO term indicates the total number of genes in that category.

<https://doi.org/10.1371/journal.pgen.1007390.g002>

evaluated Ca^{2+} dynamics and regeneration, upon addition of eATP or apyrase, an enzyme that hydrolyses ATP to AMP. Addition of eATP without injury provoked an increase of $[\text{Ca}^{2+}]_c$ (Fig 3A). However, when the mycelium was pre-treated with apyrase, the fluorescence signal after injury was abolished, as compared to an untreated (no apyrase) control (Fig 3A). Furthermore, damaged hyphae treated with apyrase showed a strongly reduced regeneration capacity (Fig 3B): only 26% of hyphae regenerated (Fig 3C). We also evaluated the transcriptional changes that occur when adding eATP; remarkably, as upon injury, we found that gene expression associated with DNA replication, the cell cycle, RNA biosynthetic processes and organic acid transport was induced (S1 Fig, S5 Dataset). Thus, ATP released from damaged cells promotes regeneration, likely by promoting calcium influxes.

Similarly, we evaluated if ROS is necessary for triggering Ca^{2+} influx and hyphal regeneration. For this purpose, we evaluated changes in $[\text{Ca}^{2+}]_c$ upon injury in presence of the antioxidant N-acetyl-Cysteine (NAC) and its analog N-acetyl-glycine (NAG), as control. After injury, a spike of $[\text{Ca}^{2+}]_c$ was observed even in the absence of ROS (NAC treatment) (Fig 3D), suggesting that ROS are not required to trigger Ca^{2+} influxes and possibly regeneration. To determine if NOX-dependent ROS production plays a role in hyphal regeneration, we performed regeneration assays using the Δnox1 , Δnox2 and ΔnoxR mutants. In all cases emergence of new hypha from the cell adjacent to the broken one was observed (Fig 3E). All mutants showed the same capacity to regenerate observed in the WT strain (Fig 3F). To explore if ROS regardless of its source played a role in regeneration, we applied a NAC treatment prior to injury, observing no difference in the percentage of regeneration compared with the untreated control (Fig 3F). These results are consistent with eATP acting as a DAMP (a form of “danger signal”), that activates a Ca^{2+} influx which is necessary for hyphal regeneration. In contrast, ROS are not involved in causing the transient elevation in $[\text{Ca}^{2+}]_c$ nor in the regeneration process.

Tmk1 is essential for hyphal regeneration

To determine if MAPK signal transduction pathways are involved in the regeneration process, we used gene replacements mutants of the MAPK encoding genes *tmk1* and *tmk3*. Hyphal regeneration in the WT, Δtmk1 and Δtmk3 strains was analyzed after damage with a scalpel. The regenerative capacity of the Δtmk1 mutant was drastically affected, since in many cases we did not observe the emergence of new hyphae (Fig 4A). On average, only 20% of the hyphae showed regeneration in the absence of Tmk1, compared with 68% in the wild type strain (Fig 4B). In contrast, the Δtmk3 mutant exhibited only a slight decrease in regenerative capacity, with 56% of the hyphae regenerating (Fig 4B).

To identify injury-responsive genes linked to MAPKs, we performed a transcriptional analysis using RNA extracted from the Δtmk1 and Δtmk3 mutants upon injury and compared their transcriptional profiles with that of the WT strain. We identified a set of Injury-Responsive Tmk1 dependent (IRK1) genes, whose expression changes upon injury in the WT and Δtmk3 strains (94 up-regulated and 127 down-regulated) were no longer observed in the Δtmk1 mutant, which shows strongly reduced regeneration (Fig 4C, S6 & S7 Datasets). These

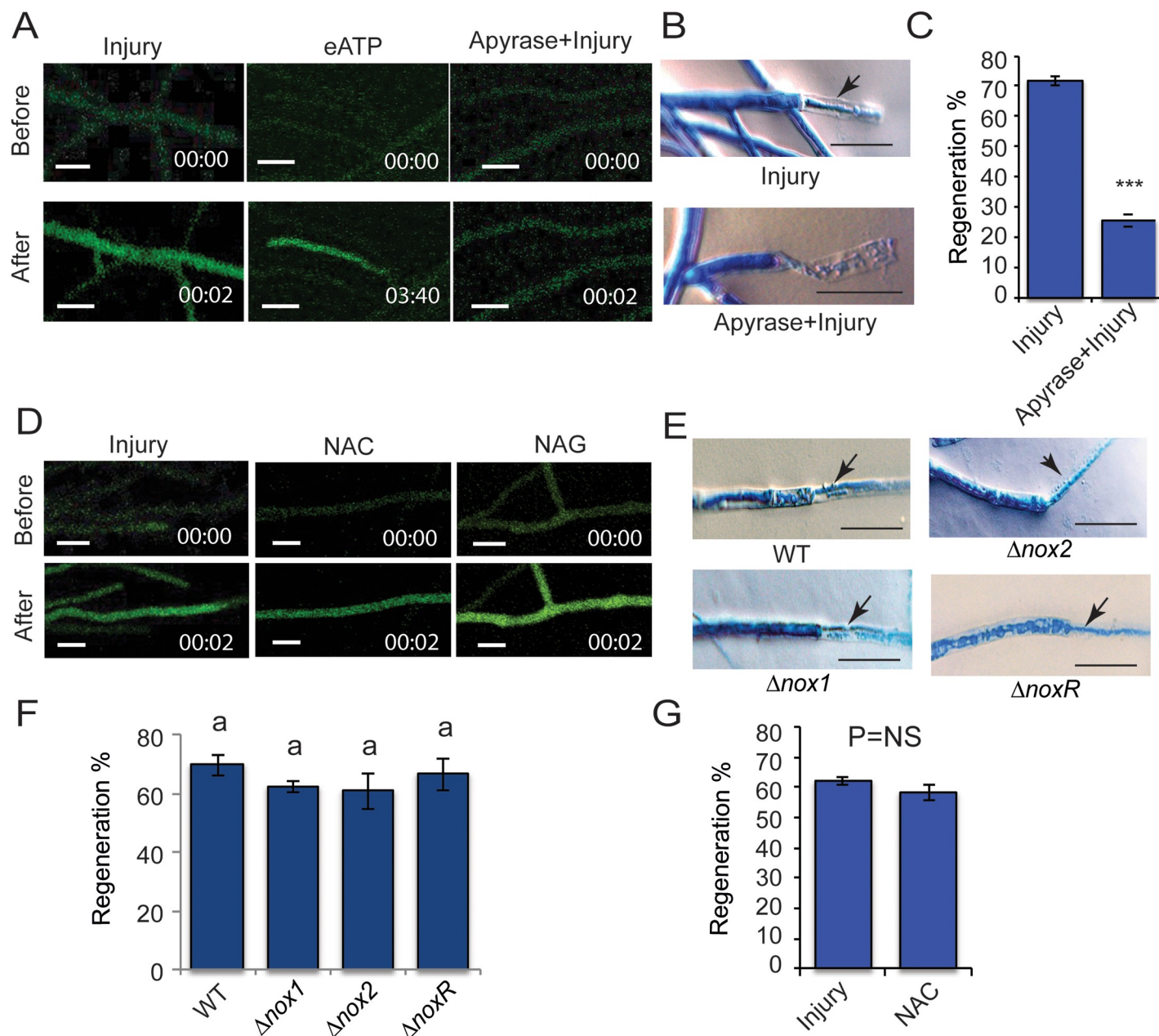


Fig 3. Role of eATP and ROS in Ca^{2+} influx and regeneration. A & D. Live-cell imaging of the *T. atroviride* WT strain carrying pEM12 treated with 100 μ M ATP (eATP) or apyrase and then injured (A) or 30 mM NAC or NAG and then damaged (D), the WT strain subjected only to injury was used as a control. Images were obtained using time-lapse confocal microscopy whilst applying the treatment. Scale bar = 10 μ M. Time shown in minutes. B & E. Microscopic changes observed after injury. The photographs in B show the response of the WT strain upon injury or treatment with apyrase for 15 min and then damaged. The images in E show the response of the $\Delta nox1$, $\Delta nox2$ and $\Delta noxR$ mutants upon damage. Hyphae were stained with lactophenol cotton blue and examined by light microscopy. Arrows point to the new regenerating hyphae. Scale bar = 10 μ M. C. The graph shows the percentage of hyphae of the wild type strain that regenerate upon injury or apyrase treatment prior to injury. G. The graph shows the percentage of hyphae of the WT strain that regenerate upon injury and those that regenerate when injured after exposure to 30 mM NAC (NAC). C & G. Bars represent the mean \pm s.e.m. A t-test was performed, with a significant ($P < 0.001^{***}$) or non-significant ($P = NS$) difference. F. The graph shows the percentage of hyphae in the $\Delta nox1$, $\Delta nox2$ and $\Delta noxR$ mutants that regenerate upon injury. Bars represent the mean \pm s.e.m. A one-way ANOVA was used. There was no significant difference between treatments ($P < 0.05$) as indicated by $P = NS$. C, F & G. Three independent experiments were performed for each treatment, counting 50 hyphae in each case. There was no difference between treatments ($P < 0.05$) as indicated by $P = NS$.

<https://doi.org/10.1371/journal.pgen.1007390.g003>

analyses clearly showed that most clusters of genes differentially expressed in both the WT and $\Delta tmk3$ strains remained nearly unresponsive in the $\Delta tmk1$ mutant (Fig 4D). The IRK1 genes

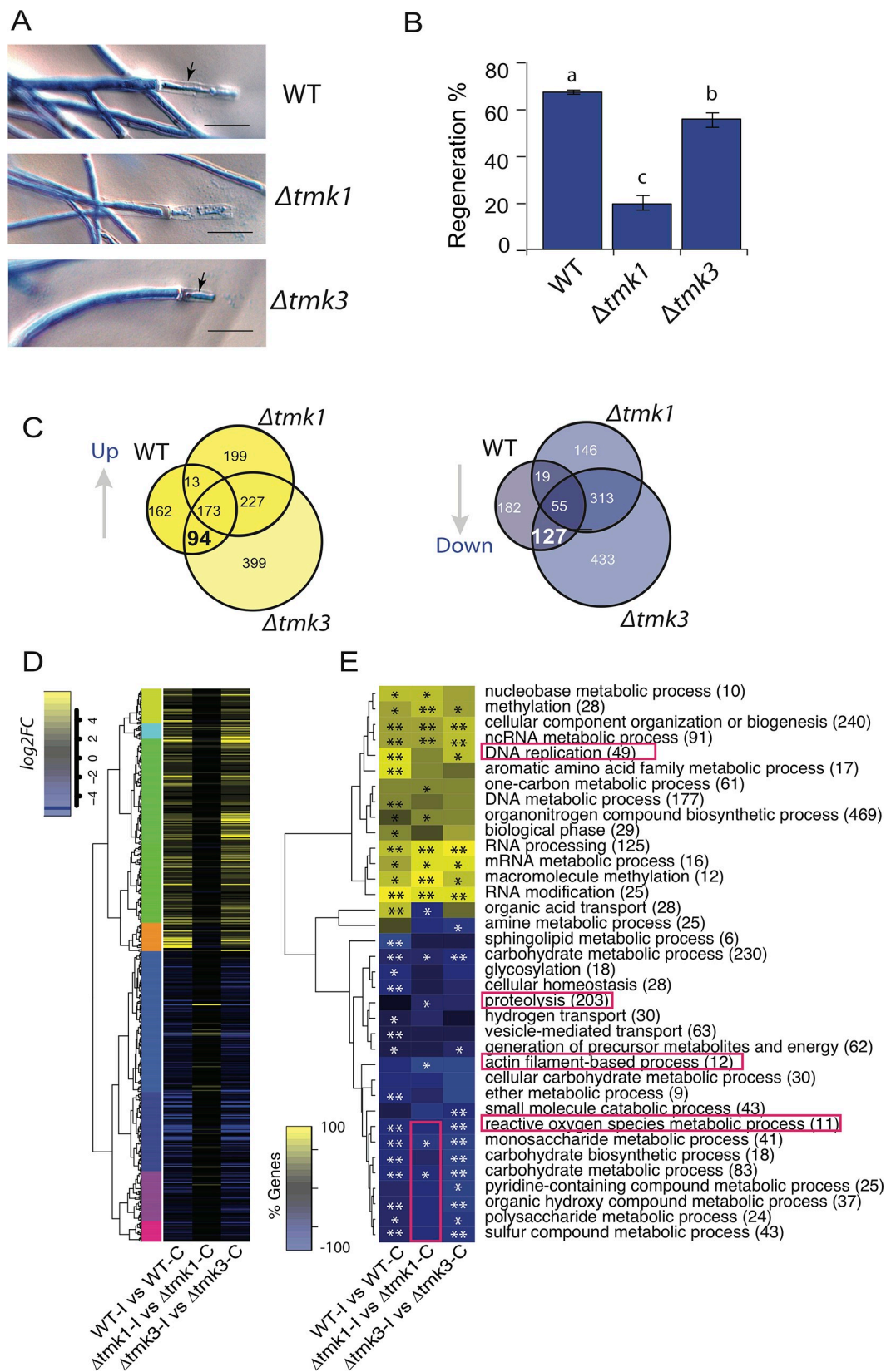


Fig 4. Tmk1 signaling is required for hyphal regeneration and correct transcriptional response. **A.** Microscopic changes observed 1 h after injury in the WT, $\Delta tmk1$ and $\Delta tmk3$. Hyphae were stained with lactophenol cotton blue and examined by light microscopy. Arrows point to the new hyphae. **B.** The graph shows the percentage of hyphae that regenerate upon injury in each strain. Three independent experiments were performed for each treatment, counting 50 hyphae in each case. Bars represent the mean \pm s.e.m. A one-way ANOVA test, followed by Tukey Honest Significant Differences was used. Different letters indicate significant differences ($P < 0.05$). **C.** Venn diagrams showing the overlap between up-regulated and down-regulated genes that respond to injury in the WT, $\Delta tmk1$ and $\Delta tmk3$ strains. **D.** Heat map showing the expression profile of the Injury-Responsive Tmk1 dependent (IRK1) genes and their behavior following injury in each strain ($FDR < 0.05$; Fold-change > 1). **E.** Heat map with enriched GO biological process terms, showing the percentage of genes belonging to each category ($FDR < 0.01^{**}$; $FDR < 0.05^{*}$). The number in parenthesis after each GO term indicates the total number of genes in each category.

<https://doi.org/10.1371/journal.pgen.1007390.g004>

included key elements of cell signaling, DNA replication, and DNA metabolic processes (S8 Dataset). The pattern of expression of the IRK1 genes in the $\Delta tmk3$ mutant was similar to that observed for the wild type strain at early stages of the response to injury. Nevertheless, we detected 13 up-regulated and 19 down-regulated genes that did not respond to injury in the $\Delta tmk3$ mutant but responded to the stimulus both in the WT and $\Delta tmk1$ strains (Fig 4C). Given that the latter strains can proceed into conidiation, this set of Injury-Responsive Tmk3 dependent (IRK3) genes might represent a set involved in the onset of conidiation (S8 Dataset).

A Gene Ontology analysis of the transcriptional response to injury in each strain suggests that the functional response in the $tmk3$ mutant is quite similar to that of the WT (Fig 4E). Although cellular component organization and RNA processing categories responded similarly in all three strains, the $tmk1$ mutant did not show a significant up-regulation of genes involved in DNA replication nor down-regulation of several metabolic processes, including that of reactive oxygen species (Fig 4E). On the other hand, genes encoding proteins associated with actin filaments and proteolysis, likely required for regeneration, were only down-regulated in $\Delta tmk1$ (Fig 4E).

Calcium signaling and the Tmk1 pathway drive expression of regeneration genes

Until now, two of our experimental conditions led to an impaired regeneration capacity after injury: $\Delta tmk1$ and WT treated with the Ca^{2+} chelator, BAPTA. We hypothesized that these facts could be used to define genes required for regeneration by comparing gene expression profiles between regenerating and non-regenerating conditions/strains: (WT injury, $\Delta tmk3$ injury) versus ($\Delta tmk1$ injury, BAPTA injury). To make sure that the resulting genes respond to injury in the WT, we then compared them with those differentially expressed in the comparison WT injury vs WT control (Fig 5A). The intersection of both groups represents what we define as the “Regeneration Associated Gene Set” (RAGS), which expression is associated with regeneration, constituted by 520 up-regulated and 466 down-regulated genes (Fig 5A). Based on Gene Ontology, the induced component of the RAGS was enriched in genes involved in DNA and RNA metabolic processes, cellular responses to stress, the cell cycle, and ribosome biogenesis, among others (S2 Fig). However, no significant functional enrichment was found for the down-regulated genes.

Closer inspection and manual annotation allowed us to classify the induced set of genes into 7 functional categories (Fig 5B, S9 Dataset). Six of the RAGS categories are involved in processes clearly associated with regeneration in many other organisms: cell proliferation (35 genes), replication (43 genes), cellular signaling (10 genes), response to stress/DNA repair (25 genes), transcription regulation (69 genes), and ribosome biogenesis/translation (36 genes). Interestingly, the seventh group (22 genes) is mostly constituted by genes related to programmed cell death and genes with a fungus-specific HET domain. Upon manual inspection

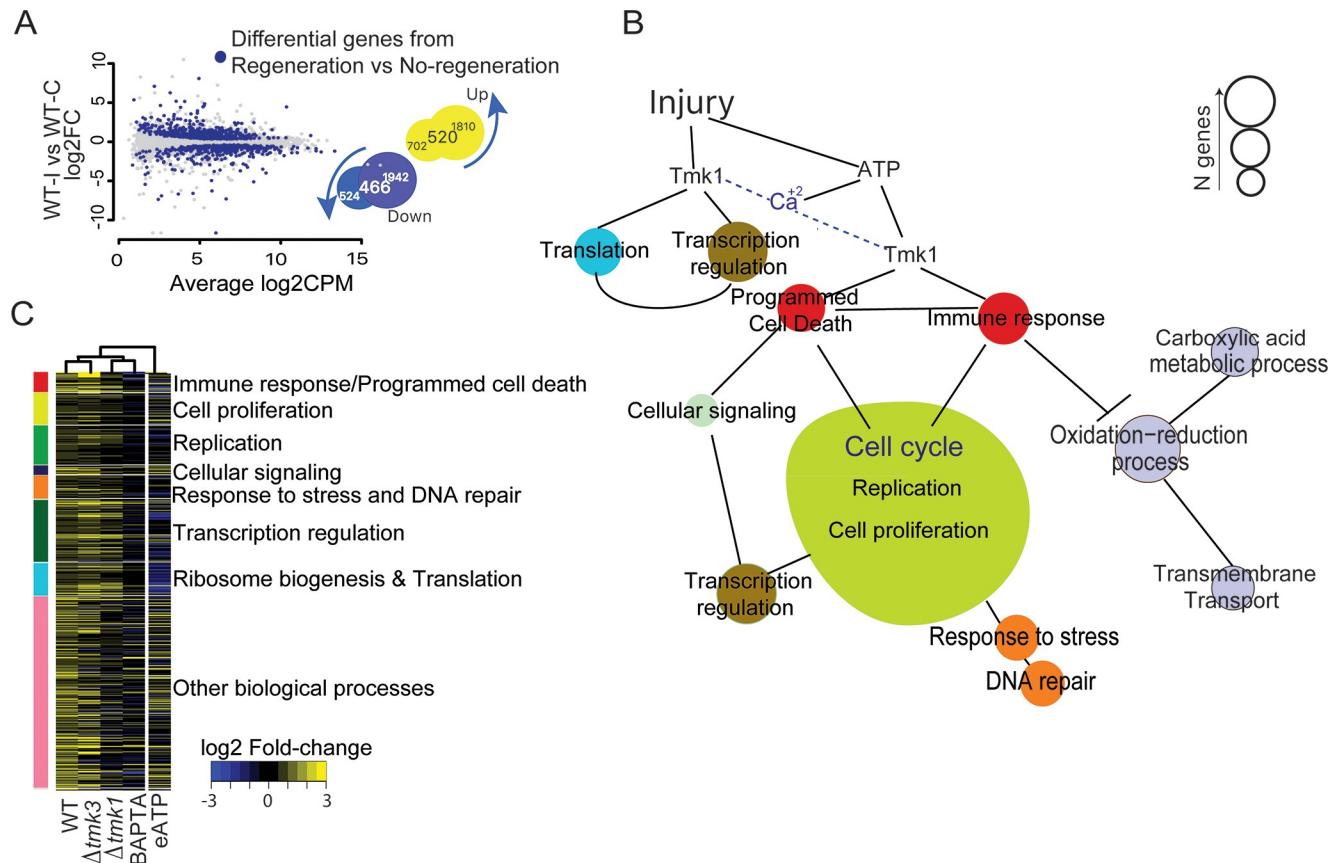


Fig 5. Functional analysis of Regeneration Gene Set. **A.** The plot highlights the differentially expressed genes from the “Regeneration vs No-Regeneration” comparison (blue dots) on the results of the WT-Injury vs WT-Control comparison. The Venn diagrams show the intersections between the two comparisons. **B.** Model based on manual inspection of regeneration genes with enriched Gene Ontology terms. Circle sizes are proportional to the number of genes contained in each category. **C.** Heatmap of the regeneration genes’ fold-change after injury in the different mutants and pharmacological treatments. Vertical color bar groups genes by GO term, colored as in B. Hierarchical clustering of columns was determined using the *hclust* function of the stats package in R, and the distance measured using a Pearson correlation and “complete” as the clustering method.

<https://doi.org/10.1371/journal.pgen.1007390.g005>

of the down-regulated RGS, we found a large number of genes involved in oxido-reduction processes (S10 Dataset).

As expected, when looking at the individual treatments/strains, we observed that the RAGS did not respond to injury or showed a strongly diminished response in the $\Delta tmk1$ mutant and upon BAPTA treatment. Instead they followed similar patterns of expression to those of the $\Delta tmk3$ and WT strains upon injury, and after addition of ATP (Fig 5C). Additionally, we observed that application of eATP mostly mimicked the response of the genes provoked by injury in the WT (Fig 5C). Interestingly, the genes of the ribosome biogenesis/translation and transcription regulation categories, which are up-regulated upon injury of the WT, are down-regulated upon treatment with eATP. These observations indicate that eATP is not sufficient to trigger a full regeneration response (Fig 5B).

To better understand the dynamics of expression of the RAGS we selected four genes belonging to three different categories, namely cell proliferation (*rad5*, Id. 172559), cell signaling (*cmk1*, Id. 301592), and programmed cell death (Het domain, Id. 294334; Nacht domain, Id. 88516) for quantitative gene expression analyses. As expected, we observed a strong increase in the level of all four transcripts early after injury, reaching their maximum at 15

min, when the new regenerating hyphae become barely visible (Fig 6). The expression of the genes clearly decreases by 30 min, when the new hyphae have already emerged (Fig 6). The level of expression of all four genes then starts dropping slowly, and 5 h after injury, when most (90%) regenerated hyphae were completely evident (Fig 6A), they reached the level observed in the control.

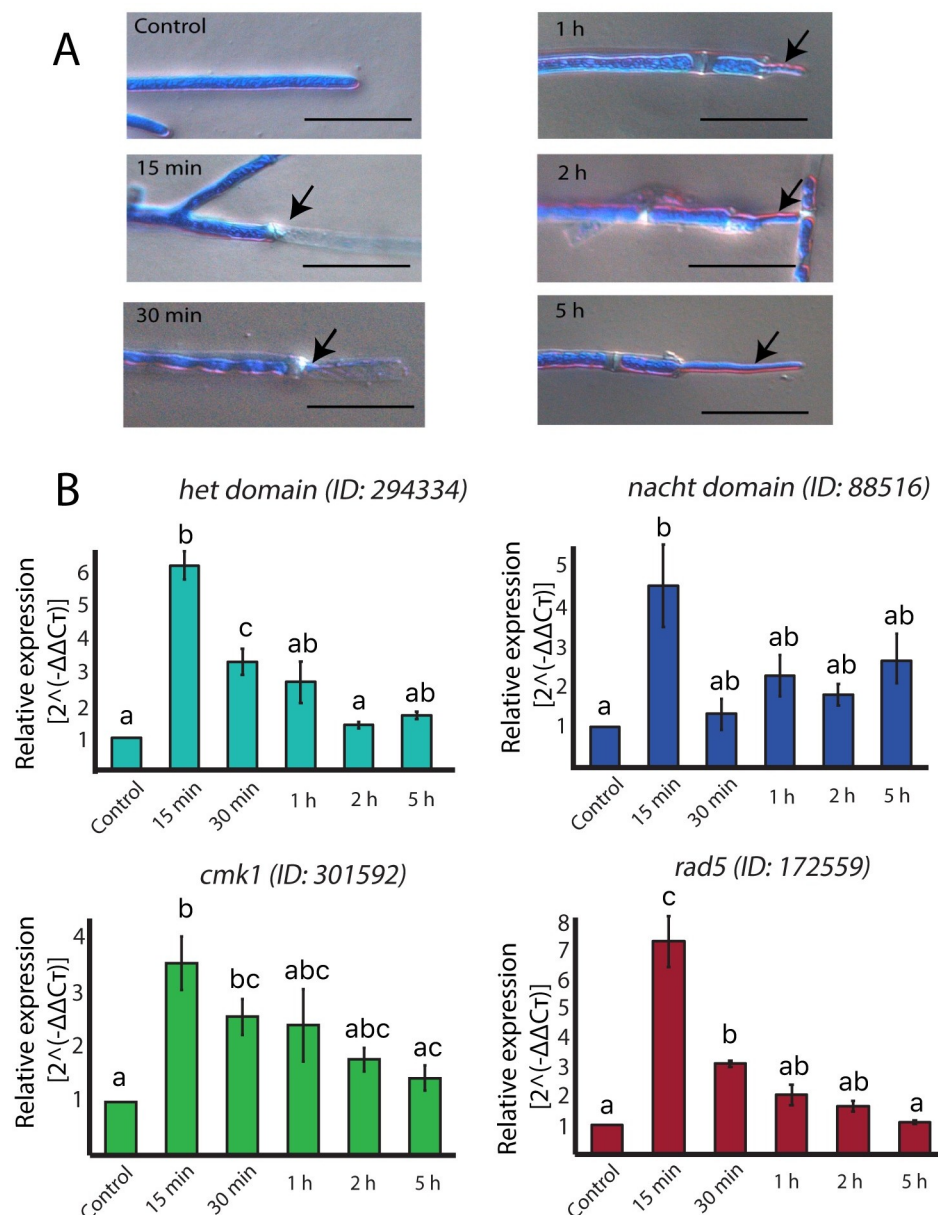


Fig 6. The expression of RGS correlates with the initial stages of regeneration. **A.** Microscopic changes observed after injury. Hyphae were stained with lactophenol cotton blue and examined by light microscopy. Regenerating hyphae were photographed 15, 30 minutes, and 1, 2, and 5 hours after injury. Scale bar = 10 μ m. Images are representative of the morphological stage of the hyphal population at the indicated time. **B.** Relative mRNA expression of a Het domain, a Nacht domain encoding genes, and the *rad5*, and *cmk1* genes. The expression is relative to DNA polymerase encoding gene (Id. 53190), which expression does not vary under the tested conditions. Graphs show the results of four biological and three technical replicates. Error bars represent \pm s.e.m. A one-way ANOVA test, followed by Tukey test were used to determine significant differences, indicated by different letters ($P < 0.05$).

<https://doi.org/10.1371/journal.pgen.1007390.g006>

Discussion

We have previously shown that *T. atroviride* responds to mycelial injury by rapidly regenerating its hyphae and, developing conidia in a Nox-dependent manner [19]. We had also shown that eATP induces conidiation and triggers activation of Tmk1 and Tmk3, and that the latter is activated in a Nox1-NoxR dependent fashion [20]. Further, mutants in either *tmk1* or *tmk3* were affected in injury-induced conidiation, which is the final outcome of the process [20]. Intriguingly, depletion of extracellular Ca^{2+} blocked injury induced conidiation but allowed activation of both MAPKs [20]. In this regard, Ca^{2+} released from a damaged cell may be detected by neighboring cells as a signal molecule or serve as a second messenger liberated from intracellular pools and/or be transported across the plasma membrane upon detection of DAMPs. However, it was unclear whether the regeneration and conidiation processes were mechanistically linked and how all these elements were interconnected to regulate the response to damage.

In this regard, two of the earliest signaling events after wounding in animals and plants are the activation of MAPKs and Ca^{2+} influxes [2]. MAPKs are also involved in the early stages of regeneration in hydra [26] and planaria [27]. Likewise, here we show that the MAPK Tmk1 is involved in hyphal regeneration control. Furthermore, $[\text{Ca}^{2+}]_c$ increases are necessary for sealing the disrupted plasma membrane [28], and Ca^{2+} signaling is essential to activate defense responses in plants and the immune system in mammals [29, 30]. Similarly, we detected a transient increase in $[\text{Ca}^{2+}]_c$ seconds after damage, which was promoted by eATP, as one of the earliest events of the response to injury with evidence that the increase in $[\text{Ca}^{2+}]_c$ is regulated by extracellular Ca^{2+} involving a mechanism known as Ca^{2+} -induced Ca^{2+} -release [31]. Interestingly, in filamentous fungi, deletion of Cch1 or Mid1, which are components of a mechanosensing Ca^{2+} -channel complex, results in diminished thigmotropic responses, and failure to establish cell polarity [32]. A comparable mechanism of mechanosensing is used by mammals during immune cell activation [33, 34]. A direct link between the increase in $[\text{Ca}^{2+}]_c$ and the control of transcription, was revealed by the up-regulation of the Ca^{2+} /calmodulin dependent kinase CAMK1, and the transcriptional factor CRZA in response to injury. In planaria and hepatic stem cells calmodulin encoding genes are induced by wounding [13, 35], and intimately linked with the signals activating the innate immune system [36]. Moreover, we found that increasing $[\text{Ca}^{2+}]_c$ and eATP are necessary for the formation of new, regenerated hyphal tips and re-initiation of mycelial growth upon injury. In this regard, it has been established that actin cytoskeleton rearrangements are Ca^{2+} -dependent and determine the site of tip growth and polarized cell movement [32, 34]. In plants and animals, ROS production is required during healing and regeneration [14, 15, 37]. In contrast, it appears that ROS are not required for hyphal regeneration, although they could participate as signal molecules in the early response inducing genes involved in injury-induced conidiation [18, 19]. This is consistent with the fact that Tmk3 is activated by ROS, both necessary for injury-induced conidiation but not regeneration [20]. Thus, as in plants and animals, signaling by eATP, Ca^{2+} and MAPKs appears to be essential for regeneration in filamentous fungi.

We further show that the Ca^{2+} and Tmk1 signaling pathways, appear to control the expression of thousands of genes. However, we defined a Regeneration Associated Gene Set (RAGS) in which these two signaling pathways converge. The RAGS could be involved in either the metabolic changes required to produce a new hypha and reinitiate growth (regeneration), respond to mechanical stress, and/or defense. Six different processes that could clearly be linked to regeneration are strongly represented within the RAGS. Some of the individual genes found within the RAGS encode proteins involved in cell cycle regulation and two components of the condensin complex, whose participation in regeneration processes has been documented [38, 39, 40]. It is noteworthy that we also found genes, such as *ssu72*, required for

replication initiation and previously shown to participate in the control of cell cycle progression in mice in response to liver damage [41]. We also found DNA replication licensing factors (*mcm* genes), which are up-regulated during regeneration in planaria, mice and axolotl [42–44], and have been shown to play a key role in cell proliferation [45].

We defined a seventh group within the RAGS, which contains eight genes encoding HET domain proteins. In this regard, fungal hyphae from different individuals can fuse, resulting in the coexistence of genetically different nuclei in a common cytoplasm (heterokaryon). The fate of the fused cell is determined by HET domain proteins through allorecognition processes, in which heterokaryons resulting from the fusion undergo a type of programmed cell death [24, 46]. In addition, we found two induced homeodomain transcription factors, annotated as potential mating type factors. In *Neurospora crassa*, some HET domain proteins interact with mating factors to carry out the heterokaryon incompatibility process. Allorecognition processes allow the distinction of self from non-self in cells and tissues, and participate in processes, ranging from tissue transplant fusion to immune defense, across the tree of life [47].

Remarkably, in addition to HET domain protein encoding genes, we found 14 genes which participate in either cell death or the innate immune system in animals. Among them a caspase, a putative phosphatidylserine-specific receptor, a PITSLRE protein kinase, and the activation of apoptosis signal-regulating kinase 1, all of which play major roles in apoptosis [48–50]. Other interesting genes within this group were a 3–5 exoribonuclease *csf4*, a probable GMP synthase, and a Ca^{2+} -independent phospholipase A2, which are key elements of the innate immune response in animals [51–53].

Fungi, like all organisms, are potential hosts for microbial pathogens and have developed defense systems against competitors and pathogens. Programmed cell death and non-self-recognition systems are considered an important strategy to contend with infections in fungi, plants and animals [16]. Furthermore, heterokaryon incompatibility has been shown to prevent various forms of somatic parasitism, and to reduce the risk of transmission of infectious cytoplasmic elements and mycoviruses [54–56]. This set of HET domain proteins together with two DEAD/H-box helicases present in our RAGS, and which have been implicated in cytosolic DNA sensing [57], could play a major role in detecting damaged or invading DNA molecules. Furthermore, in plants and animals, the innate immune response relies on specific proteins, the pattern-recognition receptors (PRRs), which detect conserved pathogen-associated molecular patterns and “danger” signals [2, 58]. The domain architecture of HET proteins is similar to that of both plant and animal cytosolic PRRs, suggesting that similar modes of activation occur even if primary sequences and downstream functions are diverse [52, 59]. These incompatibility genes are extremely polymorphic and show signatures of diversifying selection [52, 60]. Moreover, recent biochemical evidence showed that fungal NLR-like proteins function similarly to NLR immune receptors in plants and animals, concluding that NLRs are major contributors to innate immunity in three kingdoms, including fungi [59]. Consequently, HET proteins may be involved in protecting the fungus from pathogens, invading DNA/RNA molecules, and serve as damaged self-recognition system, as components of an innate immune system.

Based on these observations, we propose that a filamentous fungal innate immune response process promotes regeneration and we designate this set of 22 genes as the innate immunity group. The importance of the activation of the immune system in regeneration in organisms such as zebrafish and hydra has previously been documented [61, 62]. Thus, we postulate that there is a cellular Boolean system that determines entry into cellular proliferation, mediated by different genes involved in perception of exogenous and/or damaged genetic material, which lead to cell death if the cell/tissue damage is too extensive or caused by pathogenic organisms, since initiating DNA replication would compromise genome integrity. However, if this were

not the case, rapid communication with the DNA repair and replication systems would take place and regeneration would be promoted.

According to Sanchez-Alvarado [1], the molecular cascades associated with regeneration may have appeared first and foremost as a way to asexually propagate species, and that such cascades may have been co-opted by many organisms to cope with injury. Here we show that filamentous fungi, which have the capacity to reproduce by fragmentation, share many elements thought to be exclusively used by animals for regeneration. Furthermore, although speculative at this stage, our data suggest that in fungi an innate immune system is involved in hyphal regeneration, with the participation of HET domain proteins, previously thought to exclusively trigger programmed cell death [24]. In this regard, although the domain architecture and mechanistic functioning of NLR proteins are strikingly similar, their evolution in the different kingdoms of life is thought to be convergent [63, 64]. Thus, our findings indicate that the signaling pathways involved in regeneration across kingdoms were likely co-opted to aid this process after multicellularity evolved.

Materials and methods

Strains and culture conditions

Trichoderma atroviride IMI 206040 was used as the wild type strain (WT). The $\Delta tmk1$ and $\Delta tmk3$ mutants have been described previously [20], as have the $\Delta nox1$, $\Delta nox2$, and $\Delta noxR$ mutants [19]. The *T. atroviride* strain carrying the Ca^{2+} sensor GCaMP6 [65] (Calmodulin::GFP), was obtained by transformation with the plasmid pEM12 (see below). All strains were propagated on potato dextrose agar.

Plasmid construction

To generate pEM12, the sequence of GCaMP6 (Calmodulin::GFP) was obtained from plasmid pSK379 [66] and amplified by PCR using the primers GCaMP6-EcoRI-FW and GCaMP6-SalI-RV. *T. atroviride* was then transformed with pEM12, as previously described [67], and subjected to five passes through monospore culture. All oligonucleotides used are indicated in S1 Table.

Analysis of $[Ca^{2+}]_c$ dynamics following mycelial injury

Colonies of *T. atroviride* expressing the Ca^{2+} -sensor GCaMP6::GFP (pEM12) were grown on Vogel's minimal medium (VMM) or Potato Dextrose Broth in 0.5% agar and incubated for 36 h on glass slides (Corning). Hyphae were damaged approximately 80 μ m behind the tips of leading hyphae, using a scalpel. They were visualized using a confocal laser scanning microscope (CLSM) Olympus FluoView FV1000 (Olympus, Japan) fitted with an argon/2 ion laser (EGFP: excitation, 488 nm; emission, 510 nm). A 60 X Plan oil-immersion objective (1.42 N. A.) was used for image acquisition. Image projections consisting of stacks of images were captured at 5 min intervals and converted into movies using confocal FluoView FV1000 (Olympus Corp.) software.

To analyze Ca^{2+} fluxes during cell damage, we used the following Ca^{2+} -modulators: 5 mM verapamil, 100 μ M dantrolene, and 10 mM of cell impermeant 1,2-bis-(o-aminophenoxy)-ethane-N,N,N',N'-tetraacetic acid tetrapotassium Salt (BAPTA) (Life Technologies). The mycelium was incubated with these modulators for 15 minutes. The colonies were then damaged with a scalpel and visualized with a CLSM. To analyze the role of eATP in the promotion of Ca^{2+} fluxes, we treated the mycelium for 15 min with 2 units of apyrase (Sigma), an enzyme that hydrolyzes ATP, before damaging the cells. Confocal imaging was performed immediately

following injury or addition of 100 μ M eATP. To analyze the role of ROS, we exposed the WT strain to 30 mM N-acetyl-cysteine (NAC) or 30 mM N-acetyl-glycine (NAG) for 15 min before damage. Untreated colonies without treatment were used as controls. The fluorescence intensity was quantified per hypha using Image J software. The mean change in fluorescence measurements were made in a 50 μ m x 30 μ m region of interest drawn over 10 hyphae approximately 80 μ m back from their tips. R packages were used for statistical analysis.

Regeneration assay

Colonies of *T. atroviride* WT, $\Delta tmk1$, $\Delta tmk3$, $\Delta nox1$, $\Delta nox2$, and $\Delta noxR$ mutants were grown in half strength PDB supplemented with 1% agarose for visualization of isolated regenerating hyphae as described above and incubated for 48 h at 27°C. The wild type strain was exposed to the Ca^{2+} modulators or apyrase (Sigma), as described above. Mycelia of the different strains/treatments were then damaged with a scalpel and incubated for 5 h. Finally, the mycelium was stained with lactophenol cotton blue for 10 min. Mycelia were observed on a Leica DM6000-B microscope fitted with a 40x objective HCX PL Fluotar (0.75 N.A.) and photographed with a Leica DFC 420C camera. R packages were used for statistical analysis.

RNAseq and differential expression analysis

Mycelia of the $\Delta tmk1$, $\Delta tmk3$ and WT strains were collected 30 min following mycelial damage and frozen immediately. The WT strain was previously treated with 10 mM BAPTA or 100 μ M ATP for 15 min, as indicated. In all cases, an injured control without chemical treatment and a control without injury were included, and three biological replicates were analyzed per strain and/or treatment. Total RNA was extracted with TRIzol (Invitrogen).

Libraries for RNAseq were prepared using the TruSeq RNA library preparation protocol (Illumina). Each library was sequenced using a NextSeq500 sequencer in the 1x75 format. The 75-bp reads were pseudo-aligned to the *T. atroviride* V2 transcripts, using *kallisto* [68]. On average, 25 million reads per library were obtained with high quality (S2 Table). The RNAseq data discussed in this publication have been deposited in NCBI's Gene Expression Omnibus [69] and are accessible through GEO Series accession number GSE115811 (<https://www.ncbi.nlm.nih.gov/geo/query/acc.cgi?acc=GSE115811>).

For the differential gene expression analysis, only those genes that had at least three counts per million in at least ten libraries were considered as transcribed. All analyses were carried out using the *edgeR* package [70]. For determining differential expression between the comparisons, we used the generalized linear model (GLM) likelihood ratio test. False discovery rates (FDR) were calculated and genes with an $FDR < 0.05$ and absolute \log_2 Fold-change ≥ 1 were considered differentially expressed. Venn diagrams and heatmaps were constructed to compare the universes of differentially expressed genes using the *gplots* package in R. To identify the set of genes related to regeneration, a highly restrictive differential expression analysis was performed with a value of $FDR < 0.01$. A Fold-change cutoff was not considered in this case.

Enrichment analyses for Cellular Component and Biological Process GO terms were performed using camera, from the *edgeR* package [71]. GO terms with $FDR \leq 0.05$ were considered significantly enriched in each comparison. We have presented this data in a clustered heatmap that highlights the categories enriched with asterisks, where ** represents $FDR < 0.01$ and * $FDR < 0.05$. The plotted values are the percentage of genes belonging to each category that are deemed differentially expressed (see previous section). The GO terms were first filtered for redundancy, removing those that contained more than 1000 or less than 4 genes.

Quantitative RT-PCR

To validate the differential expression of regeneration associated genes, primers for qRT-PCR were designed to produce amplicons around 150 bp (S1 Table). cDNA was synthesized using as template RNA extracted from injured and control mycelia, and RT II SuperScript (Invitrogen) using four biological and three technical replicates. The reaction mixture for quantitative PCR was as follows: 10 μ l of SYBR green master mix (Applied Biosystems), 3 μ l of cDNA template (3ng/ μ l) and 1 μ l of each (10 μ M) of the primers. The PCR program was as follows: One cycle at 95°C for 5 min, 40 cycles at 95°C each for 30 s, at 65°C for 30 s, 72°C for 40 s. Melting curves for each product, starting from 60°C to 95°C at 0.2°C/s, produced a single melting point. All qRT-PCR reactions were repeated three times. Anova and Tuckey tests were performed to determine the significance of changes in gene expression.

Supporting information

S1 Fig. Comparative analysis of effect of ATP and injury in gene enrichment. Clustering of enriched Biological Process Gene Ontology terms in response to injury and ATP addition, showing the \log_{10} of the FDR value (FDR <0.01**; FDR <0.05*).

(TIF)

S2 Fig. Gene enrichment analysis. Biological Process GO enrichment analysis of the intersection between the up-regulated genes in response to injury in the WT strain and those up-regulated in the “Regeneration vs No-Regeneration” comparison. The result of removing redundant GO terms is shown in a semantic similarity-based network, performed with REVIGO.

(TIF)

S1 Table. List of primers used in this work. The table shows the sequences of all oligonucleotides used in this work.

(DOCX)

S2 Table. Sequencing statistics. The table shows the sequencing and alignment statistics for each of the RNAseq library used in this work.

(DOCX)

S1 Movie. Live cell imaging. The *T. atroviride* WT strain carrying pEM12 was damaged with a scalpel and visualized using a confocal laser scanning microscope fitted with an argon/2 ion laser (EGFP: excitation, 488 nm; emission, 510 nm). Image projections consisting of stacks of images were captured during a 5 min period and converted into a movie using a confocal microscope.

(MOV)

S2 Movie. Live cell imaging. The undamaged *T. atroviride* WT strain carrying pEM12 was visualized using a confocal laser scanning microscope fitted with an argon/2 ion laser (EGFP: excitation, 488 nm; emission, 510 nm). Image projections consisting of stacks of images were captured during a 5 min period and converted into a movie using a confocal microscope.

(MOV)

S1 Dataset. Annotation of genes of differentially expressed genes upon BAPTA treatment. The table is a list of genes of the WT strain exclusively responsive to injury in absence of BAPTA, those exclusive to injury in the presence of BAPTA, and those responsive in the two treatments.

(XLSX)

S2 Dataset. Differentially expressed genes in the comparison WT+BAPTA vs WT-Control. The table includes data on expression level and statistical support summary for expression differences.

(XLSX)

S3 Dataset. Differentially expressed genes in the comparison WT+BAPTA vs WT-Injury.

The table includes data on expression level and statistical support summary for expression differences.

(XLSX)

S4 Dataset. Differentially expressed genes in the comparison WT-Injury vs WT-Control.

The table includes data on expression level and statistical support summary for expression differences.

(XLSX)

S5 Dataset. Differentially expressed genes in the comparison WT-eATP vs WT-Control.

The table includes data on expression level and statistical support summary for expression differences.

(XLSX)

S6 Dataset. Differentially expressed genes in the comparison tmk1-Injury vs tmk1-Control.

The table includes data on expression level and statistical support summary for expression differences.

(XLSX)

S7 Dataset. Differentially expressed genes in the comparison tmk3-Injury vs tmk3-Control.

The table includes data on expression level and statistical support summary for expression differences.

(XLSX)

S8 Dataset. Annotation of genes of the comparison of the transcriptional response to injury of the Δtmk mutants. The table is a list of genes responsive to injury exclusively in each of the strains analyzed (WT, $\Delta tmk1$, $\Delta tmk3$) and those responsive in the WT and each of the mutants.

(XLSX)

S9 Dataset. Up-regulated Regeneration Associated Gene Set. The table lists the 9 groups of genes up-regulated during regeneration classified according to their manually curated functional annotation.

(XLSX)

S10 Dataset. Down regulated Regeneration Associated Gene Set. The table shows a complete list of genes down-regulated during regeneration and their functional annotation.

(XLSX)

Acknowledgments

We wish to thank P. Martínez, A. Muñoz, and O. A. Callejas-Negrete for technical assistance. We also wish to thank the Unidad de Microscopía Avanzada, CICESE, for access to their imaging facilities.

Author Contributions

Conceptualization: Alfredo Herrera-Estrella.

Formal analysis: Elizabeth Medina-Castellanos, José Manuel Villalobos-Escobedo, Cei Abreu-Goodger, Alfredo Herrera-Estrella.

Funding acquisition: Alfredo Herrera-Estrella.

Investigation: Elizabeth Medina-Castellanos, José Manuel Villalobos-Escobedo.

Methodology: Meritxell Riquelme, Nick D. Read, Cei Abreu-Goodger.

Project administration: Alfredo Herrera-Estrella.

Resources: Nick D. Read, Alfredo Herrera-Estrella.

Supervision: Meritxell Riquelme, Nick D. Read, Cei Abreu-Goodger, Alfredo Herrera-Estrella.

Writing – original draft: Elizabeth Medina-Castellanos, José Manuel Villalobos-Escobedo, Cei Abreu-Goodger, Alfredo Herrera-Estrella.

References

1. Sanchez Alvarado A. Regeneration in the metazoans: why does it happen? *Bioessays* 2000; 22: 578–590. [https://doi.org/10.1002/\(SICI\)1521-1878\(200006\)22:6<578::AID-BIES11>3.0.CO;2-#](https://doi.org/10.1002/(SICI)1521-1878(200006)22:6<578::AID-BIES11>3.0.CO;2-#) PMID: 10842312
2. Heil M, Land WG. Danger signals-damaged-self recognition across the tree of life. *Front. Plant Sci.* 2014; 5: 578. <https://doi.org/10.3389/fpls.2014.00578> PMID: 25400647
3. Atwal JK, Massie B, Miller FD, Kaplan DR. The TrkB-Shc site signals neuronal survival and local axon growth via MEK and P13-kinase. *Neuron* 2000; 27: 265–277. PMID: 10985347
4. Hettenhausen C, Schuman MC, Wu J. MAPK signaling: a key element in plant defense response to insects. *Insect Sci.* 2015; 22: 157–164. <https://doi.org/10.1111/1744-7917.12128> PMID: 24753304
5. Choi J, Tanaka K, Cao Y, Qi Y, Qiu J, Liang Y, et al. Identification of a plant receptor for extracellular ATP. *Science* 2014; 343: 290–294. <https://doi.org/10.1126/science.1244364> PMID: 24436418
6. Khakh BS, North RA. P2X receptors as cell-surface ATP sensors in health and disease. *Nature* 2006; 442: 527–532. <https://doi.org/10.1038/nature04886> PMID: 16885977
7. Glaser T, Resende RR, Ulrich H. Implications of purinergic receptor-mediated intracellular calcium transients in neural differentiation. *Cell Commun. Signal.* 2013; 11: 12. <https://doi.org/10.1186/1478-811X-11-12> PMID: 23414261
8. Trautmann A. Extracellular ATP in the immune system: more than just a "danger signal". *Sci Signal* 2009; 2: pe6. <https://doi.org/10.1126/scisignal.256pe6> PMID: 19193605
9. Tanaka K, Choi J, Cao Y, Stacey G. Extracellular ATP acts as a damage-associated molecular pattern (DAMP) signal in plants. *Front. Plant Sci.* 2014; 5: 446. <https://doi.org/10.3389/fpls.2014.00446> PMID: 25232361
10. de Oliveira S, López-Muñoz A, Candel S, Pelegrín P, Calado Â, Mulero V. ATP modulates acute inflammation in vivo through dual oxidase 1-derived H₂O₂ production and NF- κ B activation. *J. Immunol.* 2014; 192: 5710–5719. <https://doi.org/10.4049/jimmunol.1302902> PMID: 24842759
11. Knapp D, Schulz H, Rascon CA, Volkmer M, Scholz J, Nacu E, et al. Comparative transcriptional profiling of the axolotl limb identifies a tripartite regeneration-specific gene program. *PLoS One* 2013; 8: e61352. <https://doi.org/10.1371/journal.pone.0061352> PMID: 23658691
12. Petersen HO, Höger SK, Looso M, Lengfeld T, Kuhn A, Warnken U, et al. A comprehensive transcriptomic and proteomic analysis of hydra head regeneration. *Mol. Biol. Evol.* 2015; 32: 1928–1947. <https://doi.org/10.1093/molbev/msv079> PMID: 25841488
13. Wurtzel O, Cote LE, Poirier A, Satija R, Regev A, Reddien PW. A generic and cell-type-specific wound response precedes regeneration in planarians. *Dev. Cell* 2015; 35: 632–645. <https://doi.org/10.1016/j.devcel.2015.11.004> PMID: 26651295
14. Gauron C, Rampon C, Bouzaffour M, Ipendey E, Teillon J, Volovitch M, et al. Sustained production of ROS triggers compensatory proliferation and is required for regeneration to proceed. *Sci. Rep.* 2013; 3: 2084. <https://doi.org/10.1038/srep02084> PMID: 23803955
15. Love NR, Chen Y, Ishibashi S, Kritsiligkou P, Lea R, Koh Y, et al. Amputation-induced reactive oxygen species are required for successful *Xenopus* tadpole tail regeneration. *Nat. Cell Biol.* 2013; 15: 222–228. <https://doi.org/10.1038/ncb2659> PMID: 23314862

16. Gonçalves AP, Heller J, Daskalov A, Videira A, Glass NL. Regulated forms of cell death in fungi. *Front. Microbiol.* 2017; 8: 1837. <https://doi.org/10.3389/fmicb.2017.01837> PMID: 28983298
17. Chan JK, Glass GE, Ersek A, Freidin A, Williams GA, Gowers K, et al. Low-dose TNF augments fracture healing in normal and osteoporotic bone by up-regulating the innate immune response. *EMBO Mol. Med.* 2015; 7: 547–561. <https://doi.org/10.15252/emmm.201404487> PMID: 25770819
18. Hernández-Oñate MA, Herrera-Estrella A. Damage response involves mechanisms conserved across plants, animals and fungi. *Curr. Genet.* 2015; 61: 359–372. <https://doi.org/10.1007/s00294-014-0467-5> PMID: 25572693
19. Hernández-Oñate MA, Esquivel-Naranjo EU, Mendoza-Mendoza A, Stewart A, Herrera-Estrella AH. An injury-response mechanism conserved across kingdoms determines entry of the fungus *Trichoderma atroviride* into development. *Proc. Natl. Acad. Sci. USA* 2012; 109: 14918–14923. <https://doi.org/10.1073/pnas.1209396109> PMID: 22927395
20. Medina-Castellanos E, Esquivel-Naranjo EU, Heil M, Herrera-Estrella A. Extracellular ATP activates MAPK and ROS signaling during injury response in the fungus *Trichoderma atroviride*. *Front. Plant Sci.* 2014; 5: 659. <https://doi.org/10.3389/fpls.2014.00659> PMID: 25484887
21. Esquivel-Naranjo EU, Garcia-Esquivel M, Medina-Castellanos E, Correa-Pérez VA, Parra-Arriaga JL, Landeros-Jaime F, Cervantes-Chávez JA, Herrera-Estrella A. A *Trichoderma atroviride* stress-activated MAPK pathway integrates stress and light signals. *Mol. Microbiol.* 2016; 100: 860–876. <https://doi.org/10.1111/mmi.13355> PMID: 26878111
22. Reithner B, Schuhmacher R, Stoppacher N, Pucher M, Brunner K, Zeilinger S. Signaling via the *Trichoderma atroviride* mitogen-activated protein kinase Tmk1 differentially affects mycoparasitism and plant protection. *Fungal Genet. Biol.* 2007; 44: 1123–1133. <https://doi.org/10.1016/j.fgb.2007.04.001> PMID: 17509915
23. Gruber S, Zeilinger S. The transcription factor Ste12 mediates the regulatory role of the Tmk1 MAP kinase in mycoparasitism and vegetative hyphal fusion in the filamentous fungus *Trichoderma atroviride*. *Plos One* 2014; 9: e111636. <https://doi.org/10.1371/journal.pone.0111636> PMID: 25356841
24. Glass NL, Dementhon K. Non-self recognition and programmed cell death in filamentous fungi. *Curr. Opin. Microbiol.* 2006; 9: 553–558. <https://doi.org/10.1016/j.mib.2006.09.001> PMID: 17035076
25. Zhao F, Li P, Chen SR, Louis CF, Fruen BR. Dantrolene inhibition of ryanodine receptor Ca^{2+} release channels molecular mechanism and isoform selectivity. *J. Biol. Chem.* 2001; 276: 13810–13816. <https://doi.org/10.1074/jbc.M006104200> PMID: 11278295
26. Manuel GC, Reynoso R, Gee L, Salgado LM, Bode HR. PI3K and ERK 1–2 regulate early stages during head regeneration in hydra. *Dev. Growth Differ.* 2006; 48: 129–138. <https://doi.org/10.1111/j.1440-169X.2006.00847.x> PMID: 16512856
27. Tasaki J, Shibata N, Nishimura O, Itomi K, Tabata Y, Son F, et al. ERK signaling controls blastema cell differentiation during planarian regeneration. *Development* 2011; 138: 2417–2427. <https://doi.org/10.1242/dev.060764> PMID: 21610023
28. Cheng X, Zhang X, Yu L, Xu H. Calcium signaling in membrane repair. *Semin. Cell Dev. Biol.* 2015; 45: 24–31. <https://doi.org/10.1016/j.semcdb.2015.10.031> PMID: 26519113
29. Vig M, Kinet JP. Calcium signaling in immune cells. *Nat. Immunol.* 2009; 10: 21–27. <https://doi.org/10.1038/ni.f.220> PMID: 19088738
30. Zhang L, Du L, Poovaiah BW. Calcium signaling and biotic defense responses in plants. *Plant Signal. Behav.* 2014; 9: e973818. <https://doi.org/10.4161/15592324.2014.973818> PMID: 25482778
31. Verkhratsky A, Shmigol A. Calcium-induced calcium release in neurones. *Cell Calcium* 1996; 19: 1–14. PMID: 8653752
32. Brand A, Gow NA. Mechanisms of hypha orientation of fungi. *Curr. Opin. Microbiol.* 2009; 12: 350–357. <https://doi.org/10.1016/j.mib.2009.05.007> PMID: 19546023
33. Eguíagaray JG, Egea J, Bravo-Cordero JJ, Garcia AG. Neurotransmisores, señales de calcio y comunicación neuronal [Neurotransmitters, calcium signalling and neuronal communication]. *Neurocirugía* 2004; 15: 109–118. PMID: 15159788
34. Joseph N, Reicher B, Barda-Saad M. The calcium feedback loop and T cell activation: how cytoskeleton networks control intracellular calcium flux. *Biochim. Biophys. Acta.* 2014; 1838: 557–568. <https://doi.org/10.1016/j.bbame.2013.07.009> PMID: 23860253
35. Cimica V, Batusic D, Chen Y, Hollemann T, Pieler T, Ramadori G. Transcriptome analysis of rat liver regeneration in a model of oval hepatic stem cells. *Genomics* 2005; 86: 352–364. <https://doi.org/10.1016/j.ygeno.2005.05.001> PMID: 15993033
36. Kumar R, Tamuli R. Calcium/calmodulin-dependent kinases are involved in growth, thermotolerance, oxidative stress survival, and fertility in *Neurospora crassa*. *Arch. Microbiol.* 2014; 196: 295–305. <https://doi.org/10.1007/s00203-014-0966-2> PMID: 24570326

37. Dunnill C, Patton T, Brennan J, Barrett J, Dryden M, Cooke J, et al. Reactive oxygen species (ROS) and wound healing: the functional role of ROS and emerging ROS-modulating technologies for augmentation of the healing process. *Int. Wound J.* 2017; 14: 89–96. <https://doi.org/10.1111/iwj.12557> PMID: 26688157
38. Aono N, Sutani T, Tomonaga T, Mochida S, Yanagida M. Cnd2 has dual roles in mitotic condensation and interphase. *Nature* 2002; 417: 197–202. <https://doi.org/10.1038/417197a> PMID: 12000964
39. Hudson DF, Vagnarelli P, Gassmann R, Earnshaw WC. Condensin is required for nonhistone protein assembly and structural integrity of vertebrate mitotic chromosomes. *Dev. Cell* 2003; 5: 323–336. PMID: 12919682
40. Onsbring Gustafson H, Jamy M, Ettema TJG. RNA sequencing of stentor cell fragments reveals key processes underlying cellular regeneration. *bioRxiv* 2018;232363.
41. Kim SH, Jeon Y, Kim HS, Lee JK, Lim HJ, Kang D, et al. Hepatocyte homeostasis for chromosome ploidy and liver function is regulated by Ssu72 protein phosphatase. *Hepatology* 2016; 63: 247–259. <https://doi.org/10.1002/hep.28281> PMID: 26458163
42. Salvetti A, Rossi L, Deri P, Batistoni R. An MCM2-related gene is expressed in proliferating cells of intact and regenerating planarians. *Dev. Dyn.* 2000; 218: 603–614. [https://doi.org/10.1002/1097-0177\(2000\)9999:9999<::AID-DVDY1016>3.0.CO;2-C](https://doi.org/10.1002/1097-0177(2000)9999:9999<::AID-DVDY1016>3.0.CO;2-C) PMID: 10906779
43. Canhamero T, Reines B, Peters LC, Andrea Borrego A, Carneiro PS, Albuquerque LL, Cabrera WH, Ribeiro OG, Jensen JR, Starobinas N, Ibañez OM, De Franco M. Distinct early inflammatory events during ear tissue regeneration in mice selected for high inflammation bearing *Slc11a1 R* and *S* alleles. *Inflammation* 2011; 34: 303. <https://doi.org/10.1007/s10753-010-9235-y> PMID: 20665098
44. Monaghan JR, Athipposhy A, Seifert AW, Putta S, Stromberg AJ, Maden M, Gardiner DM, Voss SR. Gene expression patterns specific to the regenerating limb of the Mexican axolotl. *Biol. Open* 2012; 1:937–948. <https://doi.org/10.1242/bio.20121594> PMID: 23213371
45. Lau KM, Chan QK, Pang JC, Li KK, Yeung WW, Chung NY, Lui PC, Tam YS, Li HM, Zhou L. Minichromosome maintenance proteins 2, 3 and 7 in medulloblastoma: overexpression and involvement in regulation of cell migration and invasion. *Oncogene* 2010; 29: 5475–89. <https://doi.org/10.1038/onc.2010.287> PMID: 20661220
46. Paoletti M, Saupe SJ. Fungal incompatibility: evolutionary origin in pathogen defense? *Bioessays* 2009; 31: 1201–1210. <https://doi.org/10.1002/bies.200900085> PMID: 19795412
47. Boehm T. Quality control in self/nonself discrimination. *Cell* 2006; 125: 845–858. <https://doi.org/10.1016/j.cell.2006.05.017> PMID: 16751096
48. Fadok VA, Bratton DL, Rose DM, Pearson A, Ezekewitz RA, Henson PM. A receptor for phosphatidylserine-specific clearance of apoptotic cells. *Nature* 2000; 405: 85–90. <https://doi.org/10.1038/35011084> PMID: 10811223
49. Lahti JM, Xiang J, Heath LS, Campana D, Kidd VJ. PITSLRE protein kinase activity is associated with apoptosis. *Mol. Cell Biol.* 1995; 15: 1–11. PMID: 7528324
50. Song J, Cho KJ, Cheon SY, Kim SH, Park KA, Lee WT, et al. Apoptosis signal-regulating kinase 1 (ASK1) is linked to neural stem cell differentiation after ischemic brain injury. *Exp. Mol. Med.* 2013; 45: e69. <https://doi.org/10.1038/emmm.2013.134> PMID: 24357833
51. Reddy BA, van der Knaap JA, Bot AG, Mohd-Sarip A, Dekkers DH, Timmermans MA, et al. Nucleotide biosynthetic enzyme GMP synthase is a TRIM21-controlled relay of p53 stabilization. *Mol. Cell* 2014; 53: 458–470. <https://doi.org/10.1016/j.molcel.2013.12.017> PMID: 24462112
52. Rubin BB, Downey GP, Koh A, Degousee N, Ghomashchi F, Nallan L, et al. Cytosolic phospholipase A2-alpha is necessary for platelet-activating factor biosynthesis, efficient neutrophil-mediated bacterial killing, and the innate immune response to pulmonary infection: cPLA2-alpha does not regulate neutrophil NADPH oxidase activity. *J. Biol. Chem.* 2005; 280: 7519–7529. <https://doi.org/10.1074/jbc.M407438200> PMID: 15475363
53. Thery C, Zitvogel L, Amigorena S. Exosomes: composition, biogenesis and function. *Nat. Rev. Immunol.* 2002; 2: 569–579. <https://doi.org/10.1038/nri855> PMID: 12154376
54. Biella S, Smith ML, Aist JR, Cortesi P, Milgroom MG. Programmed cell death correlates with virus transmission in a filamentous fungus. *Proc. Biol. Sci.* 2002; 269: 2269–2276. <https://doi.org/10.1098/rspb.2002.2148> PMID: 12455515
55. Debets F, Yang X, Griffiths AJ. Vegetative incompatibility in *Neurospora*: its effect on horizontal transfer of mitochondrial plasmids and senescence in natural populations. *Curr. Genet.* 1994; 26: 113–119. PMID: 8001163
56. Zhang DX, Spiering MJ, Dawe AL, Nuss DL. Vegetative incompatibility loci with dedicated roles in allogognition restrict mycovirus transmission in chestnut blight fungus. *Genetics* 2014; 197: 701–714. <https://doi.org/10.1534/genetics.114.164574> PMID: 24690544

57. Dempsey A, Bowie AG. Innate immune recognition of DNA: A recent history. *Virology* 2015; 479–480: 146–152. <https://doi.org/10.1016/j.virol.2015.03.013> PMID: 25816762
58. Iwasaki A, Medzhitov R. Control of adaptive immunity by the innate immune system. *Nat. Immunol.* 2015; 16: 343–353. <https://doi.org/10.1038/ni.3123> PMID: 25789684
59. Heller J, Clave C, Gladieux P, Saupe SJ, Glass NL. NLR surveillance of essential SEC-9 SNARE proteins induces programmed cell death upon allorecognition in filamentous fungi. *Proc. Natl. Acad. Sci. USA* 2018; 115: E2292–E2301. <https://doi.org/10.1073/pnas.1719705115> PMID: 29463729
60. Bastiaans E, Debets AJ, Aanen DK, van Diepeningen AD, Saupe SJ, Paoletti M. Natural variation of heterokaryon incompatibility gene het-c in *Podospora anserina* reveals diversifying selection. *Mol. Biol. Evol.* 2014; 31: 962–974. <https://doi.org/10.1093/molbev/msu047> PMID: 24448643
61. Lai SL, Marín-Juez R, Moura PL, Kuenne C, Lai JKH, Tsedeke AT, et al. Reciprocal analyses in zebrafish and medaka reveal that harnessing the immune response promotes cardiac regeneration. *Elife* 2017; 6: e25605. <https://doi.org/10.7554/eLife.25605> PMID: 28632131
62. Wenger Y, Buzgariu W, Reiter S, Galliot B. Injury-induced immune responses in hydra. *Semin. Immunol.* 2014; 26: 277–294. <https://doi.org/10.1016/j.smim.2014.06.004> PMID: 25086685
63. Jones JD, Vance RE, Dangl JL. Intracellular innate immune surveillance devices in plants and animals. *Science* 2016; 354: aaf6395. <https://doi.org/10.1126/science.aaf6395> PMID: 27934708
64. Urbach JM, Ausubel FM. The NBS-LRR architecture of plant R-proteins and metazoan NLRs evolved in independent events. *Proc. Natl. Acad. Sci. USA* 2017; 114: 1063–1068. <https://doi.org/10.1073/pnas.1619730114> PMID: 28096345
65. Chen TW, Wardill TJ, Sun Y, Pulver SR, Renninger SL, Baohan A, et al. Ultrasensitive fluorescent proteins for imaging neuronal activity. *Nature* 2013; 499: 295–300. <https://doi.org/10.1038/nature12354> PMID: 23868258
66. Wagener J, Echtenacher B, Rohde M, Kotz A, Krappmann S, Heesemann J, et al. The putative alpha-1,2-mannosyltransferase AfMnt1 of the opportunistic fungal pathogen *Aspergillus fumigatus* is required for cell wall stability and full virulence. *Eukaryot. Cell* 2008; 7: 1661–1673. <https://doi.org/10.1128/EC.00221-08> PMID: 18708564
67. Castellanos F, Schmoll M, Martínez P, Tisch D, Kubicek CP, Herrera-Estrella A, et al. Crucial factors of the light perception machinery and their impact on growth and cellulase gene transcription in *Trichoderma reesei*. *Fungal Genet. Biol.* 2010; 47: 468–476. <https://doi.org/10.1016/j.fgb.2010.02.001> PMID: 20144726
68. Bray NL, Pimentel H, Melsted P, Pachter L. Near-optimal probabilistic RNA-seq quantification. *Nat. Biotechnol.* 2016; 34: 525–527. <https://doi.org/10.1038/nbt.3519> PMID: 27043002
69. Edgar R, Domrachev M, Lash AE. Gene expression omnibus: NCBI gene expression and hybridization array data repository. *Nucl. Acids Res.* 2002; 30: 207–10. PMID: 11752295
70. Robinson MD, McCarthy DJ, Smyth GK. edgeR: a Bioconductor package for differential expression analysis of digital gene expression data. *Bioinformatics* 2010; 26: 139–140. <https://doi.org/10.1093/bioinformatics/btp616> PMID: 19910308
71. Wu D, Smyth GK. Camera: a competitive gene set test accounting for inter-gene correlation. *Nucl. Acids Res.* 2012; 40: e133. <https://doi.org/10.1093/nar/gks461> PMID: 22638577